

## Thermal effects of AISI 304-L stainless steel after laser irradiation

### Efeitos térmicos do aço inoxidável AISI 304-L após irradiação a laser

Article Info:

Article history: Received 2023-09-01 / Accepted 2023-11-20 / Available online 2023-12-29

doi: 10.18540/jcecv19iss11pp17806



**Anderson Kenji Hirata**

ORCID: <https://orcid.org/0009-0003-1661-1164>

Instituto Federal de São Paulo, Brazil

E-mail: [anderson.hirata@ifsp.edu.br](mailto:anderson.hirata@ifsp.edu.br)

**Claudio Luis dos Santos**

ORCID: <https://orcid.org/0000-0002-0164-6837>

Instituto Federal de São Paulo, Brazil

E-mail: [claudio.luis.santos@gmail.com](mailto:claudio.luis.santos@gmail.com)

**Helder de Paula Vicente**

ORCID: <https://orcid.org/0000-0003-4494-8509>

Instituto de Estudos Avançados, Brazil

E-mail: [helder.10@hotmail.com](mailto:helder.10@hotmail.com)

**Paulo Paiva Oliveira Leite Dyer**

ORCID: <https://orcid.org/0000-0001-7110-6871>

Instituto de Estudos Avançados, Brazil

E-mail: [paulo\\_dyer@yahoo.com](mailto:paulo_dyer@yahoo.com)

**Getulio de Vasconcelos**

ORCID: <https://orcid.org/0000-0002-2943-0915>

Instituto de Estudos Avançados, Brazil

E-mail: [getuliogv@fab.mil.br](mailto:getuliogv@fab.mil.br)

#### Resumo

Deposição por Energia Direta a Laser (L-DED) é uma das técnicas de Manufatura Aditiva (MA) emergentes dos últimos anos, e é uma das tecnologias disruptivas da Indústria 4.0. A seleção de parâmetros de solda do sistema L-DED é crítica para obter os resultados desejados na deposição em metais, entretanto, devido ao comportamento não linear intrínseco do processo, as escolhas adequadas devem ser investigadas. Nesse trabalho é apresentado um arranjo experimental para estudar os efeitos térmicos em substrato de metal durante o processo de irradiação. Com 40% e 60% da potência do feixe de laser, os resultados da irradiação mostraram apenas mudanças de cor, mas nenhuma mudança na rugosidade ou poça líquida foi formada. Porém, com 68% da potência do laser, foi observado um aumento considerável da temperatura média do substrato com valores de mais de 100°C em cada trilha adjacente criada. A zona termicamente afetada (ZTA) nessa amostra é expandida em ambos comprimento e largura à medida que a temperatura aumenta, devido ao acúmulo de calor durante o processo de irradiação. Foi concluído que a temperatura no substrato e outras variáveis de processo relacionadas a serem investigadas devem ser controladas para se conseguir a formação de cordão de solda desejada.

**Palavras-chave:** Manufatura Aditiva. Deposição por Energia Direta. Processamento Laser.

#### Abstract

Laser Directed Energy Deposition (L-DED) is one of the Additive Manufacturing (AM) techniques that has emerged in recent years, and it is one of the disruptive technologies of the Industry 4.0. The selection of welding parameters of the L-DED system is critical for obtaining the desired results in

metal deposition, however, due to its intrinsic nonlinear behavior in the process, the suitable choices need to be investigated. In this work it is presented an experimental setup to study the thermal effects on the metal substrate during the process of irradiation. With 40% and 60% of laser beam power, the irradiation results showed only a change in color, but no change in roughness or melting pool was formed. However, with 68% of laser power, a considerable increase of the substrate average temperature with values of more than 100°C at each adjacent track created was observed. The heat affected zone (HAZ) in this sample is expanded in both length and width as the temperature rises due the accumulation of heat during the irradiation process. It is concluded that the temperature of the substrate and other related process variables to be investigated must be controlled to achieve the desired bead formation.

**Keywords:** Additive Manufacturing. Directed Energy Deposition. Laser Processing.

## 1. Introduction

Rapid prototyping is one of the branches of the Additive Manufacturing (AM) process, which makes it possible to create printed parts that could be used as a final product rather than just a model. Although it was developed in the 1980's, it was only recently that AM has gained popularity, due to the advantages of product development, such as time and cost reduction, human interaction, and the overall product development cycle, with the benefit of creating parts of various shape, size, and complexity, which could be very difficult to manufacture using classical techniques (Wong & Hernandez, 2012). As reported by Ford (2014), AM is not a process yet suitable for mass production, due to inherent limitations of lengthy building time (i.e., time for processing an individual part) in comparison to process that use molds and dies (which can produce a higher number of parts at a time), but it has better advantages where products require high customization, complex designs, and are made in small quantities, or they are unique parts. This could be the case of medical and dental applications, for manufacturing prosthetic limbs, dental implants, and other aiding devices. Zheng, et al. (2019) presented that remanufacturing of parts is an important strategy in the industry, since it extends the service life of machines components, but also avoiding additional resource investments and reduces the environmental impacts related to the production of a new component.

For Metal Additive Manufacturing (MAM) processes such as Laser Directed Energy Deposition (L-DED) to produce parts for aerospace and maritime industries quality assurance is required due to strict standards, which is a challenge to obtain in most related techniques since complex thermal and material transfer occur, and defects such as voids, pores and cracks are often present in the resulting parts (He *et al.*, 2022). The process of deposition of the material depends on pre-determined welding parameters, which is difficult to achieve due nonlinear behavior of chemical and physical reactions occurring during the fabrication of the part, and also suffers influences of external conditions such as environmental temperature, substrate surface characteristics. To reduce the effects of these perturbations on the process, several Artificial Intelligence (AI) techniques have been applied to control the process in a feedback loop scheme, as reported by Lhachemi *et al.* (2019), together with measuring data from sensors, resulting in a better final product. The measured data can be acquired directly from sensors (e.g., spectrum) measuring process variables (welding current or voltage, travel speed, raw material feed rate, work distance, etc.), or can be captured from cameras as images (e.g., molten pool image).

In this work, it is investigated the influence of the rising temperature of a stainless steel as substrate, caused by the laser beam used in the deposition process to fuse the metallic powder material on the sample's surface. These preliminary results will be used as data to find the optimal welding parameters and ideal conditions needed to setup online control in the L-DED process.

## 2. Experimental Setup

The following are the description of the materials and methodology used in this work for better understanding of the influences of the process variables in the results of laser beam tracks on the sample surface. Firstly, the experimental setup is presented, then L-DED process for fabricating tracks on the sample, is detailed.

### 1.1 Laser Directed Energy Deposition System

The L-DED system (Figure 1) consists of three main components, (a) the powder feeder, (b) the fiber laser generator and laser head, and (c) the robotic arm. An AT-1210 Thermach powder feeder is used to supply the metal powder material to serve as coating or as building material. The powder heat and flow rate are controlled and is outputted at the laser head nozzle. For this experiment, however, the powder feeder was kept off since the interest was on the effect of the substrate temperature rather than the deposition of material. The laser system consisted of a 1.5kW fiber laser YLR-1500 IPG Photonics of 6mm beam diameter, and a head cladding mounted on the robotic arm as an end effector. The robotic arm used to create the tracks on the sample was a Yaskawa IR25 with a YRC1000 GP25 controller.

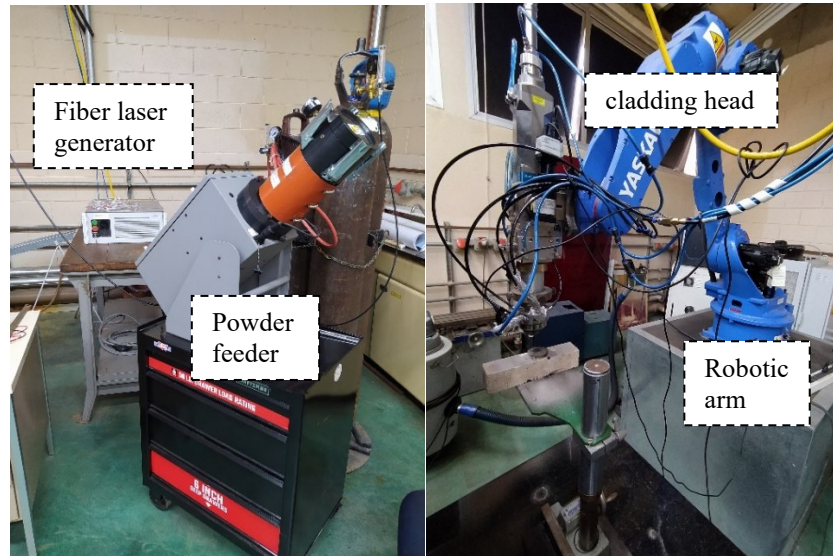


**Figure 1 - Experimental setup used in this work, showing the three main components: the powder feeder, the laser generator and cladding head, and the robotic arm.**

### 2.2 Substrate Temperature Measurement

A stainless steel sample of dimensions  $36.4 \times 29.3 \times 12.8$ mm was used as a substrate for the L-DED process test (Figure 2). In order to measure the temperature of the substrate, a thermocouple was inserted into the sample, in a cavity as small in diameter as it needed for the tip of the sensor to be allocated.

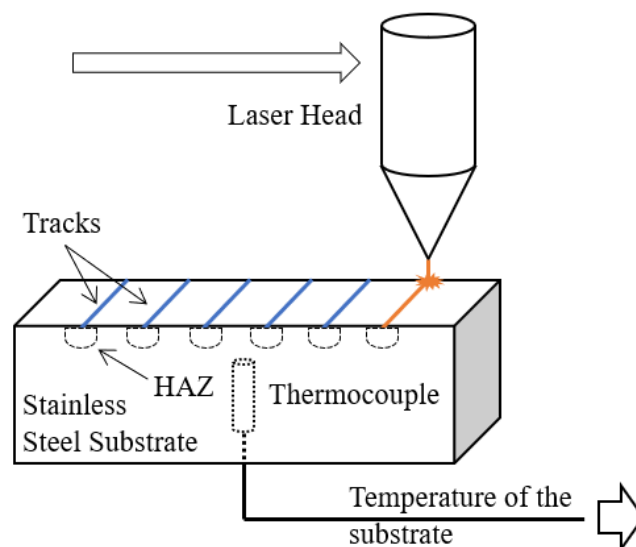


**Figure 2 - Schematic representing the experimental setup. Tracks were made on a stainless steel substrate using the laser beam while the temperature of the sample was measured.**

The robotic arm was programmed to execute a trajectory over the sample's flat surface maintaining a constant distance of 238mm in the z-axis needed for the laser focus. The laser beam was turned on from a distance of 10mm away from the side of the sample (Figure 3), then advancing at a linear trajectory at a velocity of 10mm/s, therefore creating a track (referred as TN, where N is the number of the track), then moving away at a distance of 10mm from the other side of the sample, where the laser was turned off.

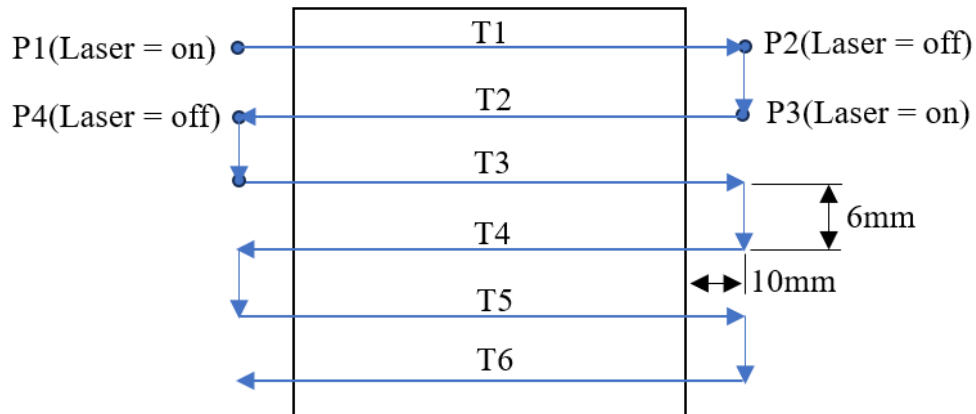


**Figure 3 - Robotic arm trajectory for creating each track in the sample.**

The average temperature of the substrate was measured before and after each track, after thermal balance. A distance of 6mm was stepped to create the adjacent track, and this procedure was kept until six tracks were made in the sample. To improve the heat exchange of the measurement system, the sample was laid on a refractory brick support, where heat transfer fins were carved out in order to minimize the contact area of the two bodies (Figure 4a). To protect the thermocouple sensor used to measure the substrate temperature, a slit was opened to give room for the instrumentation wiring.

### 3. Results and Discussion

In this section it is presented the results of the L-DED process. Four tests were conducted, with each test having an adjustment of 40%, 60% and 68% of the laser beam power ( $P_{\text{laser}}$ ), i.e., 600W, 900W and 1020W, respectively, for each sample, that is, during the fabrication of the six tracks as presented before. The evaluation of the track result was initially done qualitatively, observing if the power selection for the laser beam seemed to be causing any heat affected region at all, a possible heat affected zone (HAZ), or too much heat to the point that the track presented pool deformation along the edges, as the temperature of the substrate tend to increase with each track being fabricated.

The first test started with the laser beam power at 40% (600W) (adjusted directly from the laser generator panel) and kept constant during the track's irradiation. The result in the surface showed almost no alteration, so the second test was carried out increasing the laser beam power to 60% (900W) (Figure 4b), which presented a small change in color of the surface in comparison to the previous sample, but no apparent roughness as a bead profile formation.

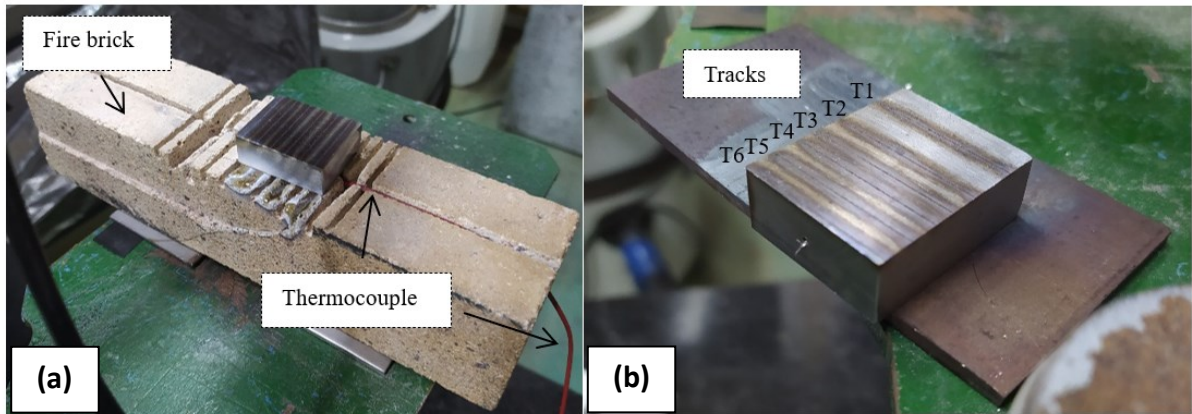


Figure 4 - Sample irradiated with laser power of 60%. (a) the sample was mounted on a refractory brick, and the thermocouple wiring was inserted into a cavity to avoid any damage that could be caused by the laser beam. (b) After the test, there were six resulting tracks, which were qualitatively evaluated together with other sensor and image data.

The third test with  $P_{laser} = 68\%$  (1020W) showed better results, but as the substrate temperature increases from track T1 to T6, the two last tracks resulted in an open molten pool, leaving raised edges along the track length. Table 1 shows the average temperature measured of the substrate for each track created at different laser beam power, and this data is presented as a plot in Figure 5.

Table 1 – Measurements results of the initial and final average temperature of the substrate sample, for each track, and laser power.

Track N°	$P_{laser} = 40\%$ (600W)		$P_{laser} = 60\%$ (900W)		$P_{laser} = 68\%$ (1020W)	
	$T_{initial} / ^\circ C$	$T_{final} / ^\circ C$	$T_{initial} / ^\circ C$	$T_{final} / ^\circ C$	$T_{initial} / ^\circ C$	$T_{final} / ^\circ C$
T1	23	46	31	71	32	100
T2	46	75	71	103	100	170
T3	75	103	103	135	170	240
T4	103	124	135	160	240	289
T5	124	138	160	189	289	323
T6	138	153	189	214	323	356

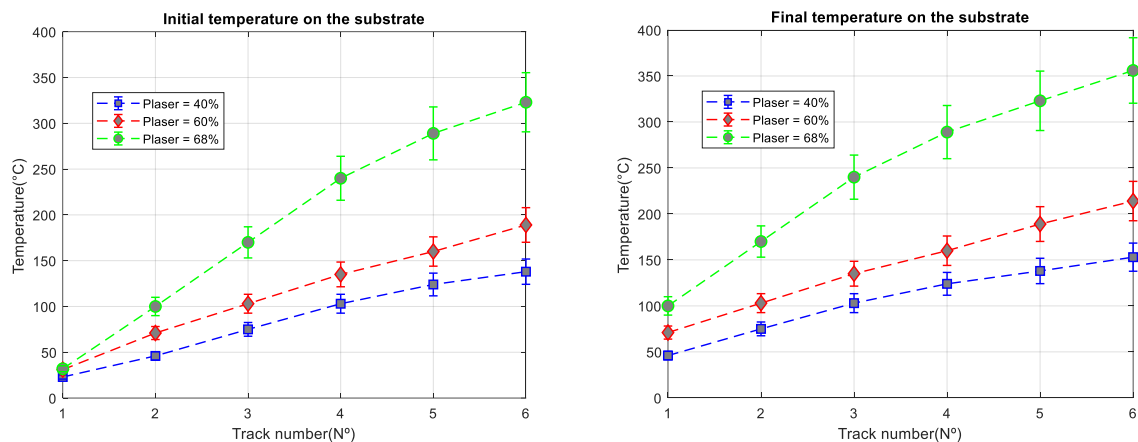
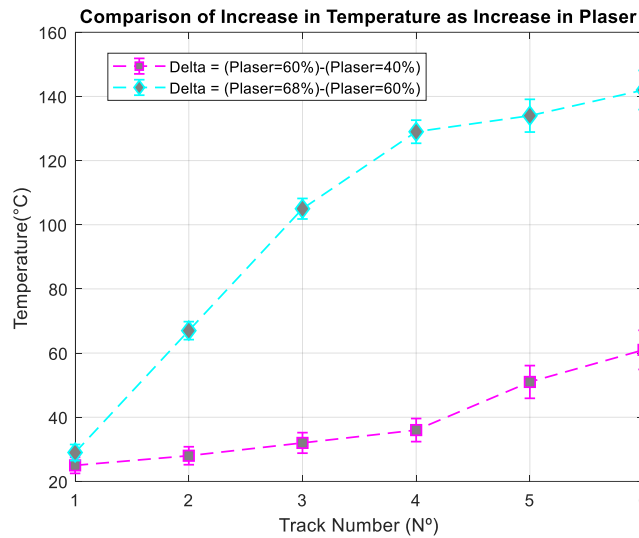


Figure 5 – Plot of the initial and final average temperature of the substrate sample, for each track, and laser power.

Figure 6 shows a comparison of the substrate temperature increase between one test to the previous one ( $\Delta T = T_{final(current)} - T_{final(previous)}$ ). An increase of laser power from 40% to 60%



(600W to 900W) showed a small increase of the substrate average temperature when the irradiation started, but the increment increases for the T5 and T6 track as more heat is accumulated in the substrate, but nevertheless, the maximum increase occurs in T6 track with a maximum of 60°C. When the laser power was increased from 60% to 68% (900W to 1020W), only the first track showed a small change of 29°C in the substrate temperature, but as the irradiation continued from T3 to T6, the values achieved were in the order of more than 100°C.



**Figure 6 - Comparison between the increase of substrate temperature as the  $P_{\text{laser}}$  increases from one test to another.**

Since the last sample with  $P_{\text{laser}}$  at 68% (1020W) showed promising results, cross-sectional images were carried out to investigate the heat affected zone of each track. Figure 7 presents the cut made in the sample, along with the images of the top and cross section of the substrate, indicating the track number associated.

From the top view images of the substrate, one can observe that as the temperature of the substrate rises, the irradiated track width increases. While the tracks T1 and T2 presented little change in roughness of the surface, the tracks T3 and T4 achieved a bead profile formation. In T5, however, the molten pool in addition to the high-pressure area created a cavity along the track with raised edges. T6 was not included in this analysis due its location to be near the end of the sample, which is difficult to separate board effects in the results.

From the cross-sectional images, it can be observed that the heat affected zone (HAZ) is expanded in both length and width as the temperature of the substrate rises due the accumulation of heat as the irradiation process is kept with constant laser power. The focused laser beam is one of the highest power density sources available in industry for welding (Steen & Mazumder, 2010), so when using laser beam as a heat source, due to this power density all materials will evaporate if the energy can be absorbed. Therefore, a hole traversing the material might be a result of this evaporation, where a high-pressure zone is formed, and the molten walls sealing up behind it. The penetration depth is inversely proportional to welding speed, focal spot size and laser beam power. Since the first and second parameters were maintained constant during the irradiation process, the temperature on the substrate due to the increased laser beam power at 68% was the responsible for the HAZ observed in Figure 8, which also shows that as the consecutive tracks were created, more heat is applied in the substrate, as mentioned earlier.

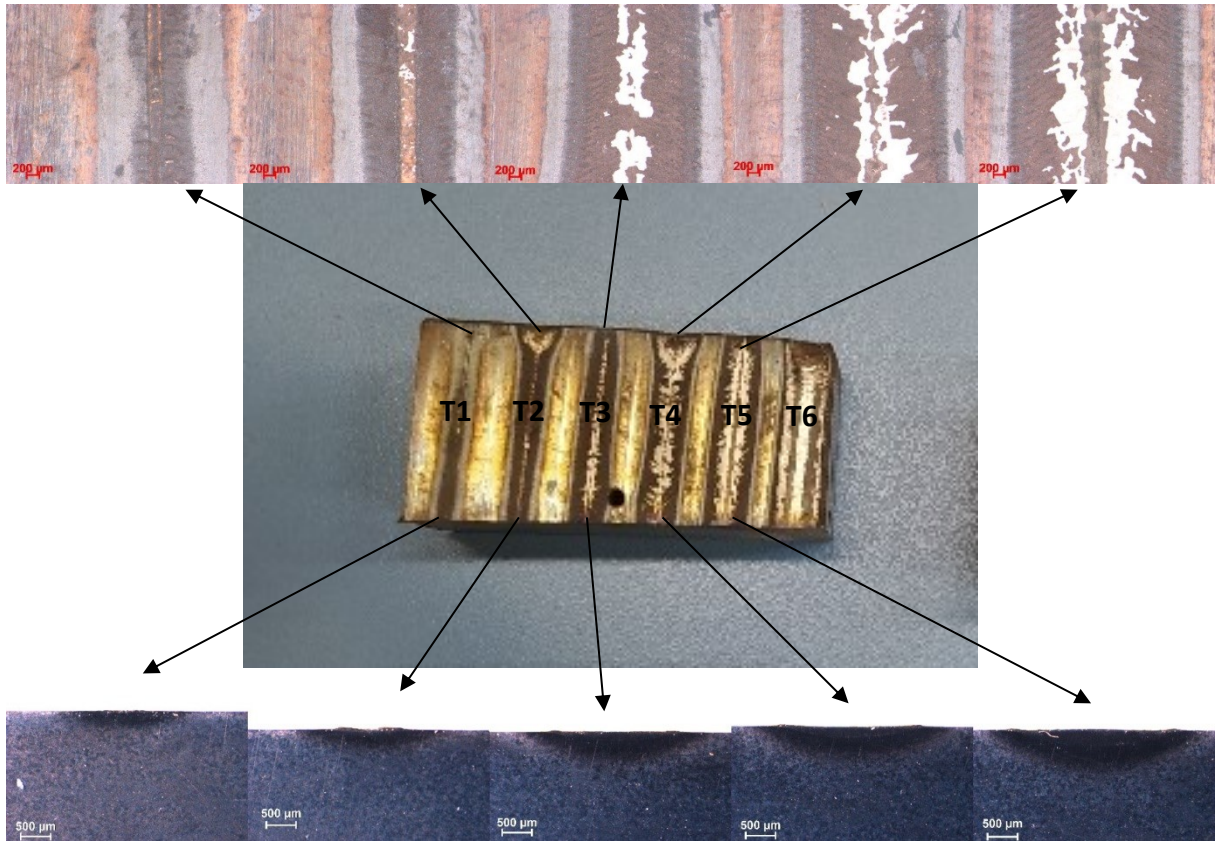


**Figure 7 - Irradiated sample with  $P_{laser} = 68\%$  that were used to obtain images of the HAZ of the tracks made from L-DED process (center). Cross-sectional view (bottom) and 3D scan (top) of stereomicroscope imaging.**

The temperature of the molten pool in L-DED process play an important role, as reported by Tang *et al.* (2020) as it affects the forming appearance of the deposited layer, with the phenomenon explained by forming failure and edge defects that occurred in a thin-wall accumulation of a cylinder cladding.

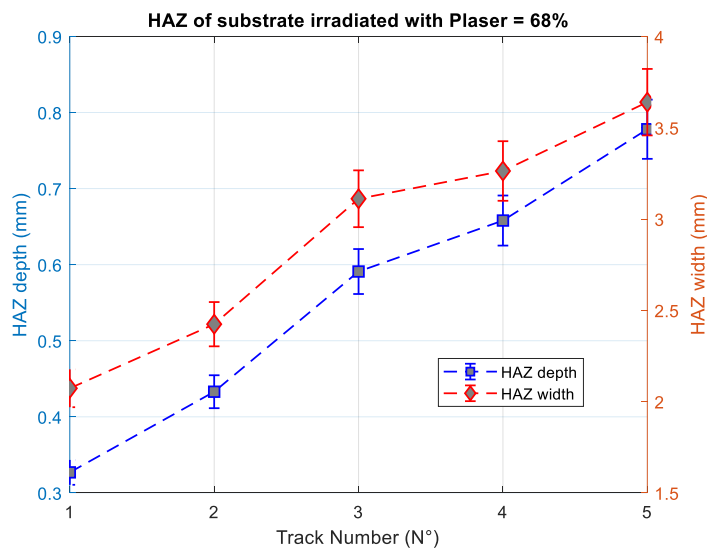


**Figure 8 - Irradiated Measure of depth and width distances of the HAZ of irradiated sample with  $P_{laser} = 68\%$  of each track made from L-DED process.**

In recent work (He *et al.*, 2023) reported several techniques, using physical sensors and melt pool image data to be used as input for online control of the deposition process, since the molten pool dynamics directly affects the results of geometry of weld beads of the final product. The

techniques involves both classical methods of process control, like the Proportional-Integral-Derivative (PID) algorithm, which uses the information of the measurements of a process variable to be controlled as input (molten pool, bead geometry data), and compared to a desired reference, it generates a control signal which manipulates another process variable (laser power, feed rate of material, velocity of displacement), but also Artificial Intelligence (AI) methods for combining different sets of data, acquired during the process and from a database, to setup the correction needed in the process. While classical PID method involves physics-based modelling of the process, which could be challenging to obtain due to the scale of nonlinearities of the relation of the input and output data while physical and chemical reactions occur in the process, the AI techniques have the advantage of being a data-driven based modelling, so as reported by Perumal *et al.* (2023) methods like Temporal Convolutional Networks (TCN) have shown promising results to be used in L-DED processes.

As the results obtained in this work showed, in order to achieve desired deposition and final product of the L-DED process, the temperature of the substrate and other related process variables must be controlled. The next steps will be to investigate in more details the relationship of the substrate temperature, molten pool data and other welding parameters used in the process, and further applying the control techniques reported in the literature.

#### 4. Conclusions

The results of temperature in a stainless steel substrate after the irradiation using the L-DED process was reported. The measured temperature data, and the analysis of the surface and cross-sectional images showed that during the process, the substrate temperature affects the bead profile and heat affected zone. In order to achieve desired results, further investigations must be conducted, so the collected data could be applied in online control techniques to adjust the welding parameters.

#### Acknowledgements

This work was funded by the Conselho Nacional de Desenvolvimento Científico e Tecnológico – Brasil (CNPq), under the grant: 405624/2022-0; Coordenação de Aperfeiçoamento de Pessoal de Nível Superior – Brasil (CAPES), under the grant: 88887.285953/2018-00, and Financiadora de Estudos e Projetos – Brasil (FINEP), under the grant: 25670-SUB-1.

#### References

- Ford, S. (2014). Additive Manufacturing Technology: Potential Implications for U.S. Manufacturing Competitiveness. *Journal of International Commerce and Economics*, 6, 1-35. Available at SSRN: <https://ssrn.com/abstract=2501065>
- He, F.; Yuan, L.; Mu, H. et al. (2023). Research and application of artificial intelligence techniques for wire arc additive manufacturing: a state-of-the-art review. *Robotics and Computer-Integrated Manufacturing*, 82, 1-20. doi: <https://doi.org/10.1016/j.rcim.2023.102525>
- Lhachemi, H.; Malik, A. and Shorten, R. (2019) Augmented Reality, Cyber-Physical Systems, and Feedback Control for Additive Manufacturing: A Review. *IEEE Access*, 7, 50119-50135. doi: <https://doi.org/10.1109/ACCESS.2019.2907287>
- Perumal, V.; Abueidda, D.; Koric, S. et al. (2023) Temporal convolutional networks for data-driven thermal modeling of directed energy deposition. *Journal of Manufacturing Processes*, 85, 105-416. doi: <https://doi.org/10.1016/j.jmapro.2022.11.063>
- Steen, W. M.; Mazumder, J. (2010). *Laser Material Processing*. Springer London.
- Tang, Z.; Liu, W.; Wang, Y. et al. A review on in situ monitoring technology for directed energy deposition of metals. *International Journal of Advanced Manufacturing Technology*, 108, 3437-3463. doi: <https://doi.org/10.1007/s00170-020-05569-3>



Wong, K. and Hernandez, A. (2012). A Review of Additive Manufacturing. *ISRN Mechanical Engineering*, 2012, 1-10.

doi: <https://doi.org/10.5402/2012/208760>

Zheng, H.; Li, E.; Wang, Y. et al. (2019) Environmental life cycle assessment of remanufactured engines with advanced restoring technologies. *Robotics and Computer-Integrated Manufacturing*, 59, 213-221.

doi: <https://doi.org/10.1016/j.rcim.2019.04.005>